communications earth & environment

Article

https://doi.org/10.1038/s43247-024-01560-y

The increasing water stress projected for China could shift the agriculture and manufacturing industry geographically

Check for updates

Mengyu Liu [1,2,3], Xiong Zhou [1,4] ✉, Guohe Huang [1] & Yongping Li[1]

The sustainable development of China has been challenged by the misalignment of water demand and supply across regions under varying climate change scenarios. Here we develop a water stress prediction index using a fuzzy decision-making approach, which analyzes spatiotemporal variations of water stress and concomitant effects on the populace within China. Our results indicate that water stress will increase from 2020 to 2099 under both low and high emission scenarios, primarily due to decreased water supplies like surface runoff and snow water content. Seasonal analysis reveals that annual fluctuations in water stress are mainly driven by changes in spring and autumn. Water stress is projected to be considerably lower in southeastern provinces compared to northwestern ones, where, on average, over 20% of the Chinese population could be severely impacted. These changes in water stress could lead to the north-to-south migration of the agriculture sector, manufacturing sector, and human population.

Water resources are essential for the development of human society[1]. However, the escalating depletion of water resources has put many parts of the world under considerable water stress[2,3], and the situations of which are estimated to much worsen due to climate change[4–6]. Under these circumstances, the growth of water-intensive sectors, such as agriculture[7,8] and manufacturing[9], will be restricted, which can potentially affect the spatial industrial layout. Therefore, it is imperative to investigate future spatiotemporal variations of water stress and to assess their impacts on industries under climate change.

Various water stress indexes (WSIs) have been proposed to estimate water stress, which is refered as the ratio of withdrawal and availability on water resouces. In general, water resources withdrawal is typically defined as the consumption of water resources for agriculture, industry, and residential sectors, while the definition of water resources availability has often been limited to river discharge[1,10,11]. Several studies have also incorporated other factors, such as environmental flow requirements, upstream consumptive water resources withdrawal, blue and green water components, to more accurately estimate WSI values[10–14]. For instance, Liu et al.[13] calculated WSI by factoring in local runoffs, environmental flow requirements, and upstream water resources withdrawals; spatial and temporal changes of water stress in China for the next three decades were then forecasted. Munia et al.[14] analyzed the impact of local runoff, inflows from upstream, and upstream water resources consumption on magnitudes of WSI globally. He et al.[15] estimated global urban WSI and witnessed a marked increase in water stress from 2016 to 2050. Incorporating blue and green water components, Liu et al.[16] estimated the agricultural water scarcity around the globe and found that more than 42% of total croplands will experience water scarcity in the future.

The per capita water resources in China are only one-fourth of the world average[17,18], which greatly hinders its sustainable development[19,20]. The geospatial distribution of water resources in China does not align with the distribution of water demands[21]. In particular, the northern regions of China have fewer water resources than the southern parts[22], but maintain more agricultural and manufacturing industries[23,24], resulting in a local water deficit, which is partly compensated by water supply from the South-to-North Water Diversion Project (SNWDP). Such a mismatch between water supply and demand could impede the development of the agriculture and manufacturing sectors is in China[25–27]. Therefore, industrial migration stands as a potential pivotal mechanism for improving the redistribution of resources[28,29], thereby facilitating the allocation of water resources across various regions. Consequently, a future redistribution of agriculture and manufacturing sectors is conceivable.

However, the commonly used WSI calculation is simplistic and may have computational deficiencies. It performs best when data are complete

[1]State Key Joint Laboratory of Environmental Simulation and Pollution Control, School of Environment, Beijing Normal University, Beijing, 100875, China. [2]College of Environmental Sciences and Engineering, Peking University, Beijing, 100871, China. [3]Department of Geography and Environment, London School of Economics and Political Science, London, WC2A 2AE, United Kingdom. [4]Faculty of Engineering and Applied Science, University of Regina, Regina, Saskatchewan, S4S 0A2, Canada. ✉e-mail: zhou.xiong@outlook.com

and precise, but in reality, water resource data derived from model calculations often entail uncertainties and ambiguities. One approach is to incorporate water resource data obtained from a greater variety of models during the calculation process. Additionally, it is necessary to employ methods capable of effectively handling data uncertainties to reconstruct the calculation of water stress.

Moreover, there have been few reports on the migration of agriculture and manufacturing sectors over China caused by water stress variations under climate change. At this juncture, scientific evidences are urgently needed to rectify the incongruity between the supply and demand of water resources.

Therefore, the objective of this study is to develop the fuzzy technique for order preference by similarity to the ideal solution water stress prediction (FTOPWSP) index. This index is intended to analyze spatiotemporal variations of water stress and their concomitant effects on the populace within China under climate change. The ensuing discussions will be further delved into the potential impacts of such variations on migration of the agriculture sector, manufacturing industry, and human population. In terms of marginal contribution, the FTOPWSP index we constructed can complement the method for calculating water stress within the overall water risk framework in the widely utilized AQUEDUCT tool developed by the World Resource Institute[30], while alleviating the ambiguities and uncertainties during the calculation of water stress. The objectives of this study entail: (i) The selection of ten water demand and supply indexes (WDSIs), including both anthropogenic and natural driving factors for water stress variations. (ii) The computation of the weight attributed to each WDSI, reflective of its influence magnitude on water stress variations.(iii) The amalgamation of the distances from each WDSI to respective fuzzy positive-ideal solution and fuzzy negative-ideal solution, thereby establishing the FTOPWSP index. (iv) The determination of a threshold of FTOPWSP in order to calculate water-stressed population (FWSPOP). (v) The examination of the implications induced by water stress variations on the migration of the agriculture sector, manufacturing industry, and human population. The results derived from these steps indicate that water stress will increase in China from 2020 to 2099. Northwestern provinces, where over 20% of the total Chinese population would be severely water-stressed, are projected to have considerably higher water stress than the southeastern ones. The projected increasing water stress and its uneven spatial distribution could lead to the north-to-south migration of the agriculture sector, manufacturing sector, and human population.

Results

The increase of future water stress over China

The annual water stress variations in China from 2020 to 2099 is estimated (Fig. 1a). The values of FTOPWSP index are projected to increase under both RCP2.6 and RCP6.0 scenarios, indicating increases in water stress in the forthcoming eight decades. Under the RCP2.6 scenario, the Sen's slope value of the FTOPWSP index is significantly positive (5.9×10^{-6}), which shows that the FTOPWSP value in 2099 would increase by 0.078% compared with that in 2020. Conversely, under the RCP6.0 scenario, the Sen's slope is not statistically significant; however, its positive value (11.3×10^{-5}) indicates an increase by 0.18% in FTOPWSP. The average of future annual FTOPWSP under RCP2.6 scenario (0.57) is smaller than that under the RCP6.0 scenario (0.58), implying that the water stress under RCP6.0 is higher than that under RCP2.6. Moreover, the spatial differences in annual FTOPWSP index values between two scenarios are projected to be quite large, as seen from the large relative differences between the 25th and 75th percentiles in Fig. 1a.

The uneven spatial distribution of water stress over China

Figure 2 and Fig. 3 show the spatial distribution of water stress over China in the mid-century (2020–2059) and late-century (2060–2099) periods. The spatial distributions of water stress in the historical period (2006–2019) are shown in Supplementary Fig. 1 and Supplemantary Fig. 2. Under both scenarios, the northern and western regions are projected to experience higher water stress than their southern and eastern counterparts. From north to south, moving from high to low latitudes, China's water stress exhibits a trend of initially increasing and then decreasing. As a result, mid-latitude regions experienced more pronounced water stress compared to those at higher and lower latitudes, with the North China Plain (NCP) facing especially large water stress. The results also indicate that from west to east, moving from lower to higher longitudes, China's water stress first decreases and then increases. This suggests that both the water-scarce western region and the high water-use eastern region experience quite large water resource stress. From Figs. 2a, b, 3a, b, the area around the Tibetan Plateau, known as Asia's water tower, exhibits very low water stress in High Mountain Asia. This further confirms the crucial role of the glacial melt of Asia's water tower in alleviating water stress[31–33]. However, it is worth noting that the terrestrial water storage of the Tibetan Plateau is facing a continuous deficit caused by global warming, which diminishes the water resources sustainability of Asia's water tower[34]. Figures 2c, d, 3c, d depict the spatial variations in water stress at the mid-century and late-century relative to the historical period under the RCP2.6 and RCP6.0 scenarios. The figures reveal that changes in water stress are more pronounced in the late-century, with the primary increase in water stress originating from Jiangsu, Anhui, and Jiangxi provinces in the East China region, as well as Hubei and Hunan provinces in the Central China region.

Hotspots and provincial distribution of FTOPWSP index

Z-scores of the Getis-Ord hotspot analysis from ArcGIS reveal the spatial cluster of the FTOPWSP index with high or low values. Figure 4 shows the hotspot analysis of late-century water stress under the RCP6.0 scenario, while the analysis under the RCP2.6 scenario can be seen in the Supplementary Fig. 3. According to the relationship between Z-score value and confidence level (Supplementary Table 2), the hot spots of FTOPWSP index are the grid clusters with high FTOPWSP index values, namely the regions with significantly high water stress. On the contrary, the cold spots are grid clusters with low FTOPWSP index values, which are the regions with significantly low water stress. Under both scenarios, cold spots would be mainly distributed in the southern parts of China. To be specific, the cold spots with more than 95% confidence are projected to be mainly located in the south, namely Zhejiang, Fujian, Jiangxi, Hunan, Guangdong, Guangxi, Sichuan provinces, as well as Asia's water tower in the Tibet, which further highlight the glacier melt's potential in reducing water stress[35]. Hot spots with more than 95% confidence would mainly be distributed in the NCP, namely Beijing, Tianjin, Hebei, Shandong, Henan, Anhui and Jiangsu, indicating a severe water stress situation in the most fertile agricultural regions in China.

Consistent with the spatial distribution of water stress, the provinces with the highest water stress were projected to be in the northern parts of China and the NCP, while those with the lowest water stress would be in the southeastern parts under both scenarios. We calculate the FTOPWSP index value for each province in the late century. The twelve provinces with the highest water stress under the RCP6.0 scenario are projected to be Tianjin (0.60), Beijing (0.596), Shandong (0.591), Jiangsu (0.589), Hebei (0.587), Henan (0.585), Shanghai (0.584) which are all in or near the NCP, and Xinjiang (0.586), Ningxia (0.586), Liaoning (0.585), Inner Mongolia (0.584), and Shanxi (0.583), which are all located in the northern China. The net annual changes in FTOPWSP index values of these regions were estimated to be positive, indicating increasing water stress in these provinces in the late century. Across these provinces, on average, the net increase in water stress throughout the year is primarily driven by an increase in water stress during the spring and winter seasons. In other words, for these provinces, there is a considerable rise in water resource stress during the winter and spring.

Seasons primarily contributing to annual changes in FTOPWSP index value

China has a monsoon climate with four distinct seasons. The climate in winter is dry and cold, which is controlled by the northerly monsoon from

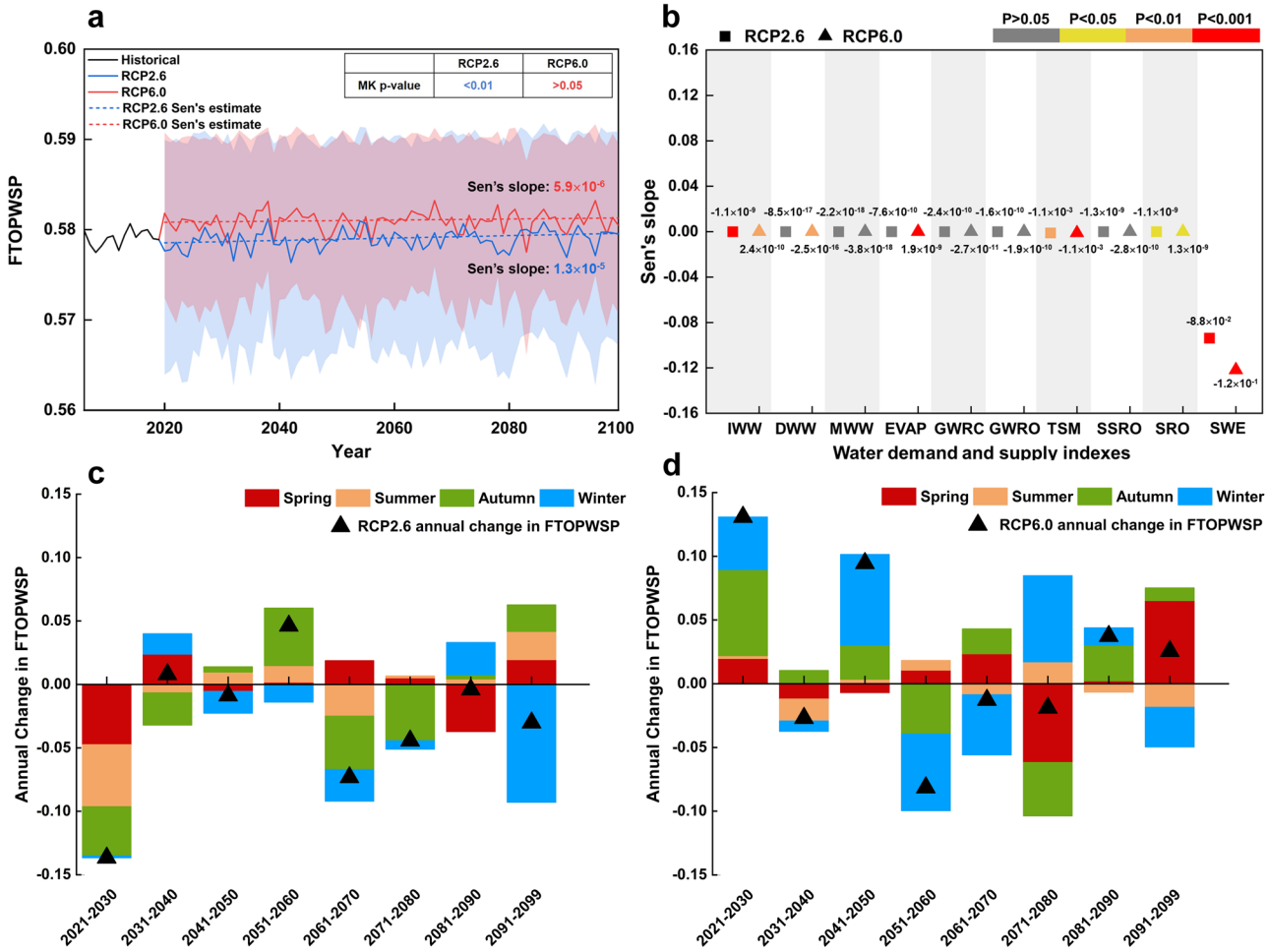

Fig. 1 | Temporal variations of water stress in China. a Annual average FTOPWSP index values in China from 2006 to 2099. The blue and red shaded areas represent the interquartile range (spanning from the 25th to the 75th percentiles) of FTOPWSP indexes under the RCP2.6 and RCP6.0 scenarios, respectively. The FTOPWSP index has an increasing trend under both RCP2.6 and RCP6.0 scenarios, indicating a growth in water stress in the forthcoming eight decades. **b** Changing trend of WDSIs. IWW refers to irrigation water withdrawal. DWW refers to domestic water withdrawal. MWW refers to manufacturing water withdrawal. EVAP refers to evapotranspiration. GWRC refers to groundwater recharge resources. GWRO refers to groundwater runoff. TSM refers to total soil moisture content. SSRO refers to subsurface runoff. SRO refers to surface runoff. SWE refers to the snow water equivalent. Decreases in water supply would drive the increases in water stress. **c** Seasonal changes in FTOPWSP index value in different decades under the RCP2.6 scenario. **d** Seasonal changes in FTOPWSP index value in different decades under the RCP6.0 scenario.

high latitudes, while that in summer is humid and rainy, which is mainly affected by the southerly monsoon from the ocean. Affected by the interaction of the above two monsoons, China's spring and autumn are transition seasons, whose temperature alternates between hot and cold with frequently changing rainfall. Under RCP2.6 scenario, the changes of water stress in spring and autumn contributed the most to the annual variations (Fig. 1c). From 2031 to 2040, and 2051 to 2080, the changes of FTOPWSP index value in autumn occupied the largest portion of total annual changes. While from 2021 to 2030, and 2081 to 2090, the changes of index value in spring contributed the most to the annual variations. Different from the RCP2.6 scenario, in most decades, the changes of FTOPWSP index value in winter contributed the most to the annual variations under the RCP6.0 scenario (Fig. 1d). This may be because that compared to the RCP2.6 scenario, under the RCP6.0 scenario, the future temperature increase will be higher, and in consequence the changes in snow water equivalent were projected to be larger (see Supplementary Table 1, which shows that the snow water equivalent index had the third largest weight, so it had a quite large impact on variations of water stress). Similar to the RCP2.6 scenario, the annual changes of FTOPWSP index value under RCP6.0 demonstrate a fluctuating trend, and the comparatively big increase in water stress under the RCP6.0 scenario are projected to occur from 2021 to 2030, and 2041 to 2050.

Primary driving factors of increasing water stress

Under both RCP2.6 and RCP6.0 scenarios, the increases in water stress were mainly driven by the decreasing water supply. Sen's estimate was conducted to reveal the changing trend of water demand and supply indexes (WDSIs) (Fig. 1b). The calculation results show that all water supply indexes had negative Sen's slopes under both scenarios, and those of the total soil moisture content, surface runoff, and snow water equivalent are statistically significant, driving the increases in water stress. The differences in water stress levels between RCP2.6 and RCP6.0 scenarios mainly stem from the different changing trends of the irrigation water withdrawal (IWW) index. Under the RCP6.0 scenario, the Sen's slope of the IWW index was significantly positive, triggering the increase in water stress. While under the RCP2.6 scenario, the IWW index's Sen's slope was significantly negative, which could contribute to the decrease in water stress. Since IWW has the largest impact on water stress variations (see Supplementary Table 1, IWW has the largest weight among all the WDSIs), IWW index emerges as the crucial factor responsible for the higher water stress under RCP6.0 scenario compared to the RCP2.6 scenario.

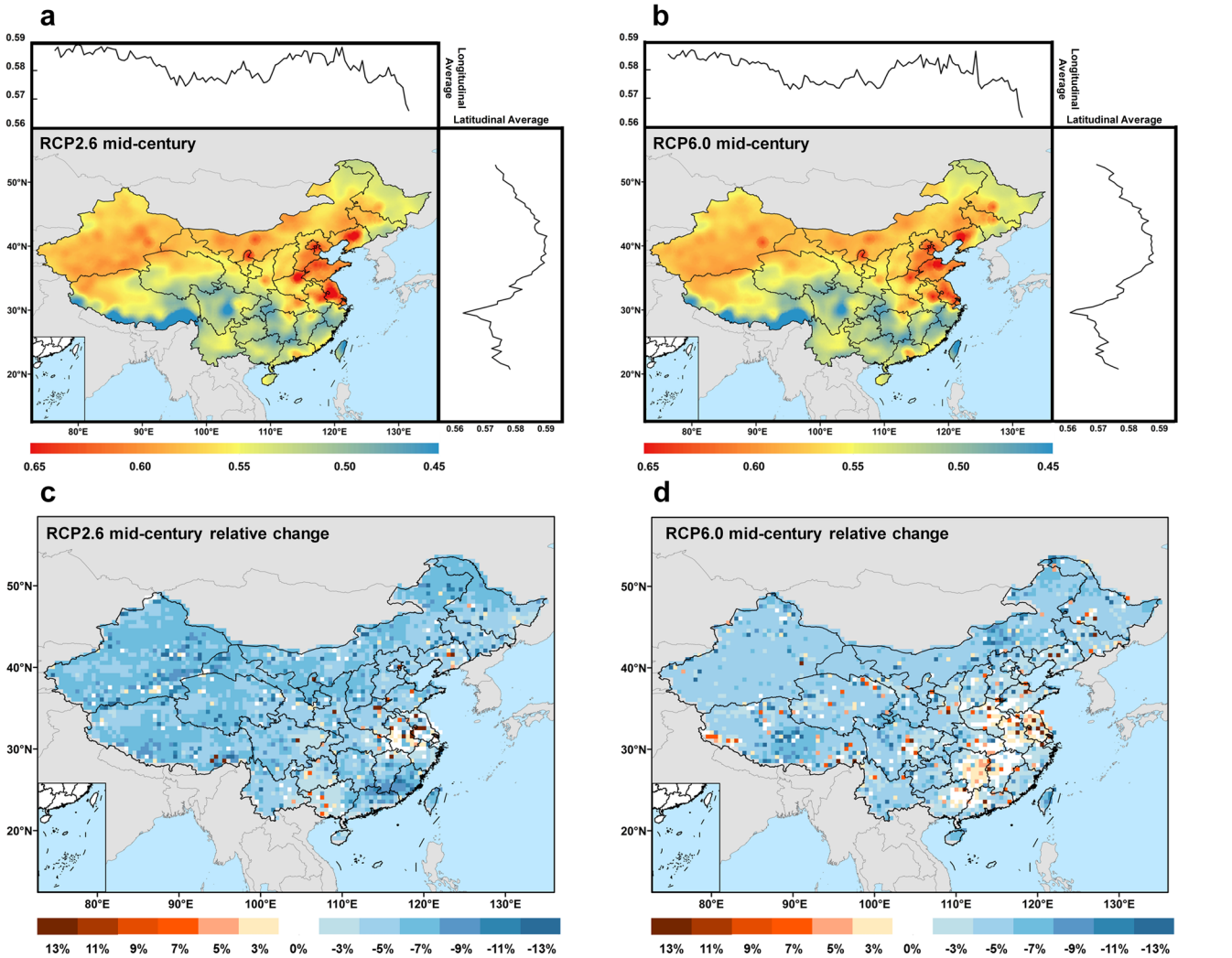

Fig. 2 | Mid-century spatial variations in water stress across China. a Spatial variations of FTOPWSP index under the RCP2.6 scenario. **b** Spatial variation of FTOPWSP index under RCP6.0 scenario. **c** Spatial distribution of mid-century water stress changes compared to historical levels under the RCP2.6 scenario. **d** Spatial distribution of mid-century water stress changes compared to historical levels under the RCP6.0 scenario.

The temporal and spatial distribution of water-stressed population

According to the future spatiotemporal distribution of water stress projected above, increasing water stress in China would have adverse impacts on human society, which might limit industries' water utilization, and higher water stress in northern and western China might drive people in these areas migrating to the south and east. To analyze and quantify water stress's impacts on humans, the 60 percentile is set as the threshold of the FTOPWSP index value. If the FTOPWSP index value of a unit grid is above the 60 percentile value, the human population in this unit grid will be considered as the water-stressed population (FWSPOP), which means that the people in this grid are affected by comparatively severe water stress. Total population data are projected by the Socioeconomic Data and Application Center (SEDAC) under the SSP2 scenario. Hence, herein, we compute the water-stressed population under the coupled RCP-SSP scenarios. Under both RCP2.6-SSP2 and RCP6.0-SSP2 scenarios, it is projected that on average, more than 20% of the total population would be affected by water stress annually (Fig. 5a). Before 2080, the FWSPOP is projected to peak in 2060 under RCP2.6-SSP2 scenario, with 49% of total population being water-stressed in 2040. While after 2080, the FWSPOP was projected to decrease. On average, 27% of the population in China would be water-stressed every year under the RCP2.6-SSP2 scenario. Under the RCP6.0-SSP2 scenario, on average, approximately 32% of the total population would be water-stressed, which is larger than that under the RCP2.6-SSP2 scenario. Besides, under the RCP6.0-SSP2 scenario, the FWSPOP would peak in 2040, with 37% of total population being water-stressed. In conclusion, there would be more people be water-stressed under the RCP6.0-SSP2 scenario.

The spatial distributions of FWSPOP are also projected. Because the spatial distribution is similar across all time periods, here only analyzes the distribution for the year 2099. (Fig. 5b, c). Under both scenarios, the water-stressed population would mainly be distributed in the northern parts of China, concentrated in eastern regions with middle latitudes. To be specific, in RCP2.6-SSP2 scenario, the longitudinal and latitudinal range of the top 20% grids with the highest FWSPOP values would be 111°E-119°E, 123°E-126°E, 26°N-27°N, and 33°N-36°N (Fig. 5b). While in RCP6.0-SSP2 scenario, the distributions of the top 20% grids with the highest FWSPOP value would be in 111°E-120°E, 27°N, 34°N-37°N (Fig. 5c). In conclusion, under both scenarios, people living in northern parts of China would be severely water-stressed in the future.

Hotspots and provincial distribution of water-stressed population

Similar to the analysis of FTOPWSP hot spots, the Getis-Ord hot spot analysis of FWSPOP is also conducted. Figure 5d shows the Getis-Ord hotspot analysis results in the late century under the RCP6.0-SSP2 scenario. The hot spots of FWSPOP are the grid clusters with high FWSPOP values,

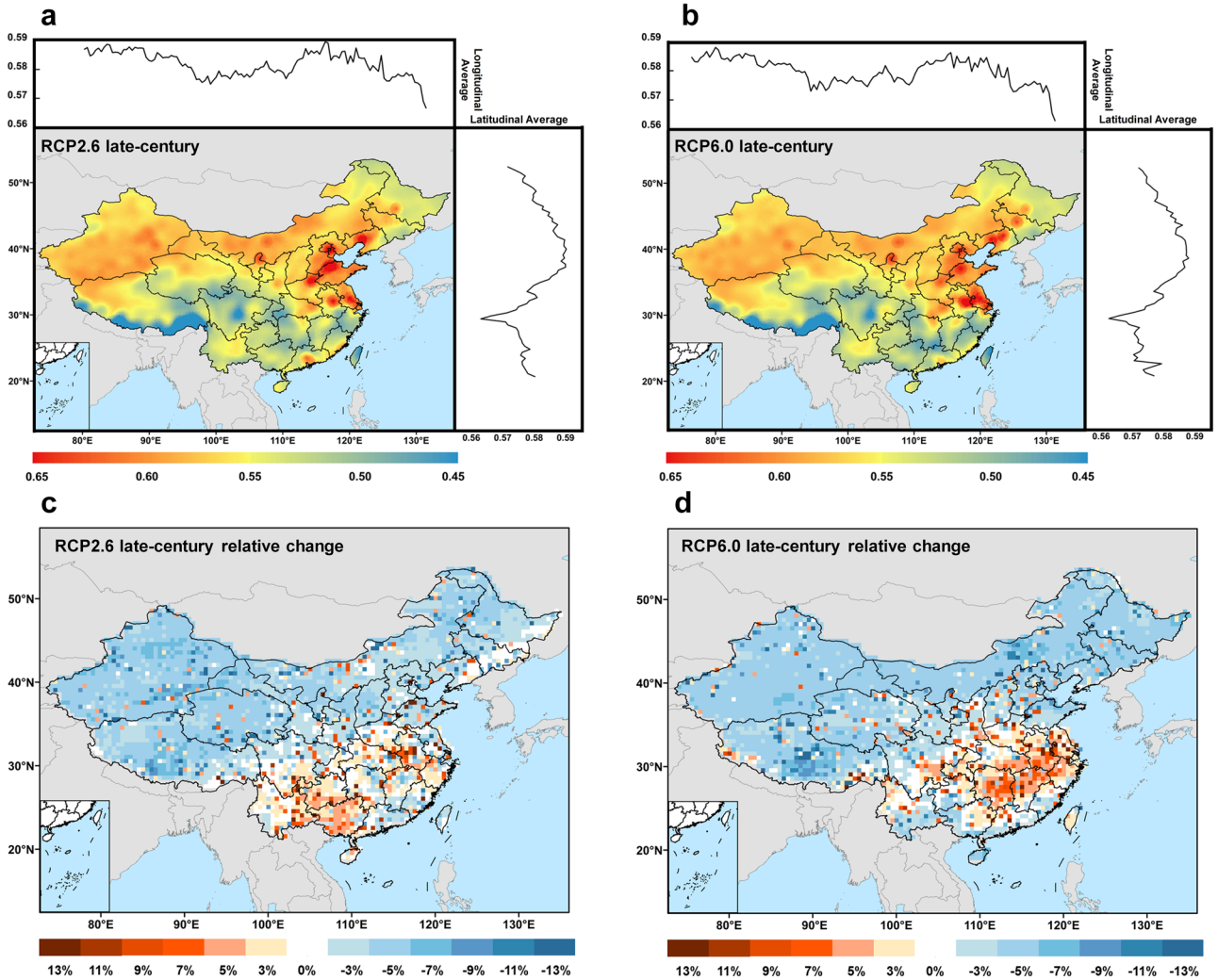

Fig. 3 | Late-century spatial variations in water stress across China. a Spatial variations of FTOPWSP index under the RCP2.6 scenario. **b** Spatial variation of FTOPWSP index under RCP6.0 scenario. **c** Spatial distribution of late-century water stress changes compared to historical levels under the RCP2.6 scenario. **d** Spatial distribution of late-century water stress changes compared to historical levels under the RCP6.0 scenario.

namely the regions with a significantly large number of water-stressed population. Conversely, the cold spots are grid clusters with low FWSPOP values, which are the regions with significantly small number of water-stressed population. The estimated Z-score results indicated that under both scenarios, the hot spots with 99% significance would be mainly located in Beijing, Tianjin, Hebei, Shandong, Henan, Jiangsu and Anhui provinces, because these areas would have both high population density and comparatively high level of water stress. The twelve provinces with the largest value of FWSPOP in late-century are projected to be mainly located in the northern parts of China or NCP, namely Shandong, Henan, Anhui, Jiangsu, Hubei, Hunan, Guangxi, Xinjiang, Gansu, Inner Mongolia, Jilin, and Heilongjiang (Fig. 4d). From the surrounding bar charts of Fig. 4d, the FWSPOP of these provinces in 2099 would be less than that in 2020 in these provinces, which is mainly due to the decreasing total Chinese population.

Discussion

We introduced an index to measure water stress, and analyzed the spatiotemporal variations of water stress in China under future climate change scenarios. We also utilized the widely adopted Water Stress Index (WSI), defined as the demand for water divided by the availability of water, to calculate the spatiotemporal variations in water stress. We found that the computational outcomes of the FTOPWSP index are highly consistent with those of the WSI, both in terms of temporal trends and spatial distribution. Supplementary Fig. 5 reveals that under the estimation of both the WSI and FTOPWSP methodologies, water stress exhibits an increasing trend, and the water stress under the RCP6.0 scenario generally exceeds that of RCP2.6. Moreover, under both methodologies, the Sen's slope calculated for the RCP2.6 scenario is statistically significant. Supplementary Fig. 6 demonstrates that the geographical distribution of water stress calculated through the WSI index aligns closely with the results from the FTOPWSP calculation. Regions experiencing high water stress are predominantly located in the northern, northwestern, or NCP areas. The high degree of consistency between the WSI and FTOPWSP calculation results attests to the reliability of our computational findings.

Meanwhile, our study has some common conclusions with other previous studies, which can further demonstrate the reliability of the FTOPWSP index. In terms of temporal variations of water stress, there would be a tendency for China's water stress to increase in the future[4,13,36]. And as for spatial variations, water stress in the northern parts of China would be larger than the southern areas[13], with the NCP facing particularly severe water stress and uneven water stress distribution[4]. Moreover, there would be over 20% of the total Chinese population under severe water stress[13,37], and the water-stressed population would be mainly concentrated in metropolis in the NCP, namely Beijing and Tianjin[15]. In addition to these common conclusions, we also find that the variations of water stress in spring and autumn would contribute the most to the annual variations.

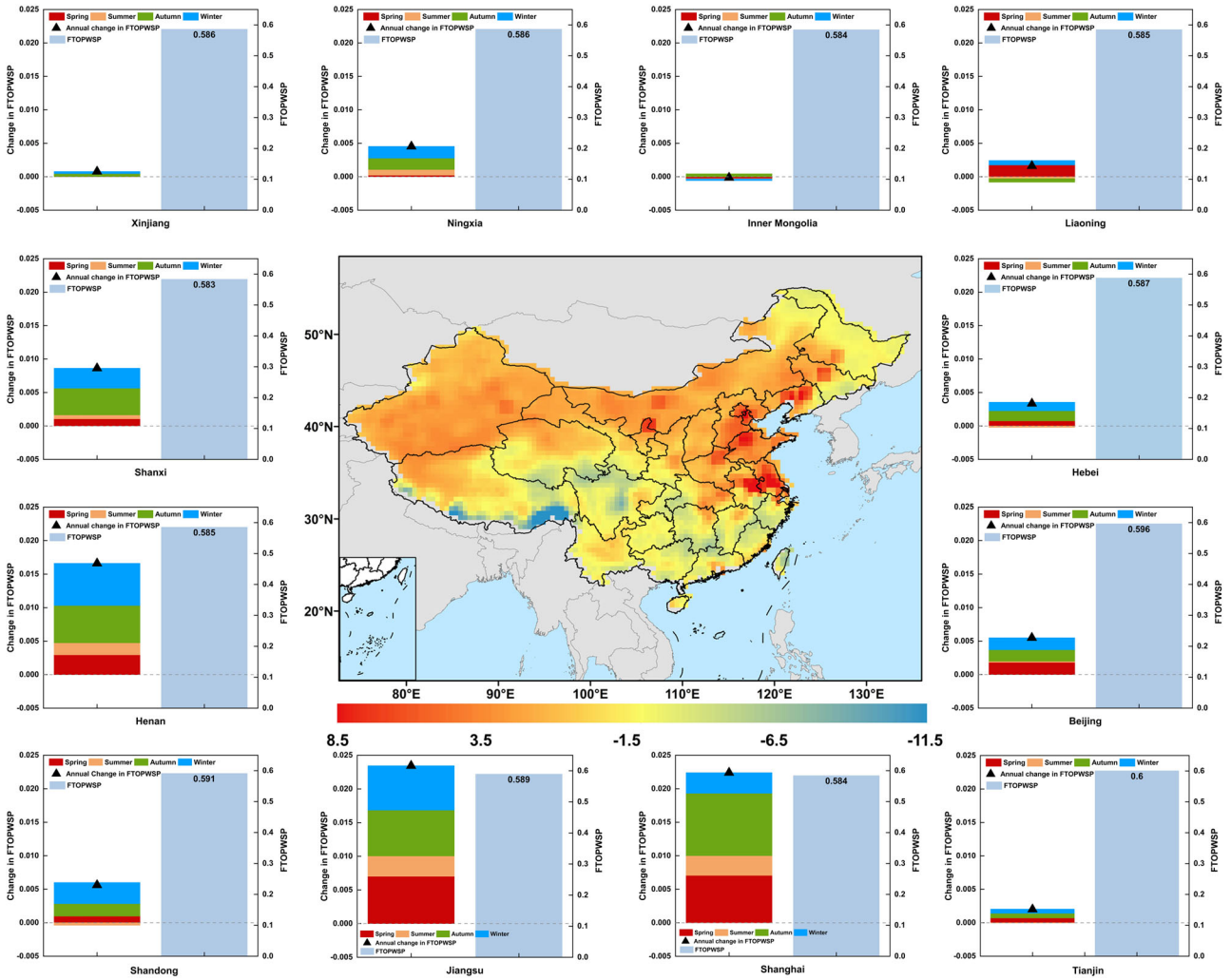

Fig. 4 | Hotspot analysis of late-century water stress under RCP6.0 scenario. The central map represents the spatial distribution of Z-score values from Getis-Ord hotspot analysis. The hot spots of FTOPWSP index are the grid clusters with high FTOPWSP index values, which are the regions with significantly high water stress. In contrast, the cold spots are grid clusters with low FTOPWSP index values, which are the regions with significantly low water stress. Surrounding bar charts represent the provincial average FTOPWSP values, seasonal changes, and net annual changes of water stress. The twelve provinces with the highest water stress levels are Tianjin, Beijing, Shandong, Jiangsu, Hebei, Henan, Shanghai, Xinjiang, Ningxia, Liaoning, Inner Mongolia, and Shanxi.

And our prediction of water stress consolidates the idea that glacier melts from Asia's water tower could help alleviate water stress[31–33] though the increasing snowmelt would be unsustainable[31]. Crucially, the FTOPWSP index, developed through the application of the fuzzy TOPSIS method, introduces an innovative strategy for alleviating the ambiguity and uncertainty inherent in calculating water stress[38]. This index also exhibits enhanced adaptability and flexibility, particularly through customizable parameters like weights, which can be tailored according to the unique data traits of diverse regions. Such adaptability facilitates bespoke evaluations for varied management aims and policy contexts. Given that the fuzzy TOPSIS method can account for multiple dimensions influencing water stress concurrently, it opens avenues for integrating considerations like water quality, population growth rate, economic development level, and water resource management efficiency into one-framework calculations in future endeavors. In addition, some models currently provide a more detailed breakdown of water demand and supply sources. For example, the H08 model can provide updated data for aqueduct water transfer, local reservoirs, seawater desalination, renewable groundwater, and non-renewable groundwater[39,40]. The classifications of detailed water supply sources in the water resources prediction models are inconsistent due to their different focuses. In order to include data from as many models as possible, we have not incorporated these more detailed sources (e.g., aqueduct water transfer)[41,42] identified by the H08 model into the current FTOPWSP calculation. However, in China, the aquatic water transfer achieved through the SNWDP is a very important source of water supply for the northern regions. Therefore, our current results may overestimate and underestimate the water stress in the north and south, respectively. In our study, the FTOPWSP approach promises a more holistic assessment of water stress's spatiotemporal dynamics and its socio-economic impacts. Based on the water resource supply and usage data in China, we identify the impacts of WDSIs on the FTOPWSP index by calculating the weight of each WDSI, and among all the water resources demand indexes, irrigation water resources withdrawal and manufacturing water resources withdrawal indexes have the largest weights (Supplementary Table 1), which indicated that these two factors had comparatively large impacts on water stress variations. Meanwhile, the irrigation water resources withdrawal index has relatively high future changing rate (Fig. 1b), indicating that it may be more sensitive to climate change, which further suggests that people would be more sensitive to adjust their water use in agriculture sectors in the face of future climate change. Therefore, combined with our findings of the uneven spatial distribution of water stress, future high levels of water stress in northern China might promote some migrations of agriculture and manufacturing sectors from north to south, which would in turn alleviate water stress in the northern parts and benefit the development of these two industries.

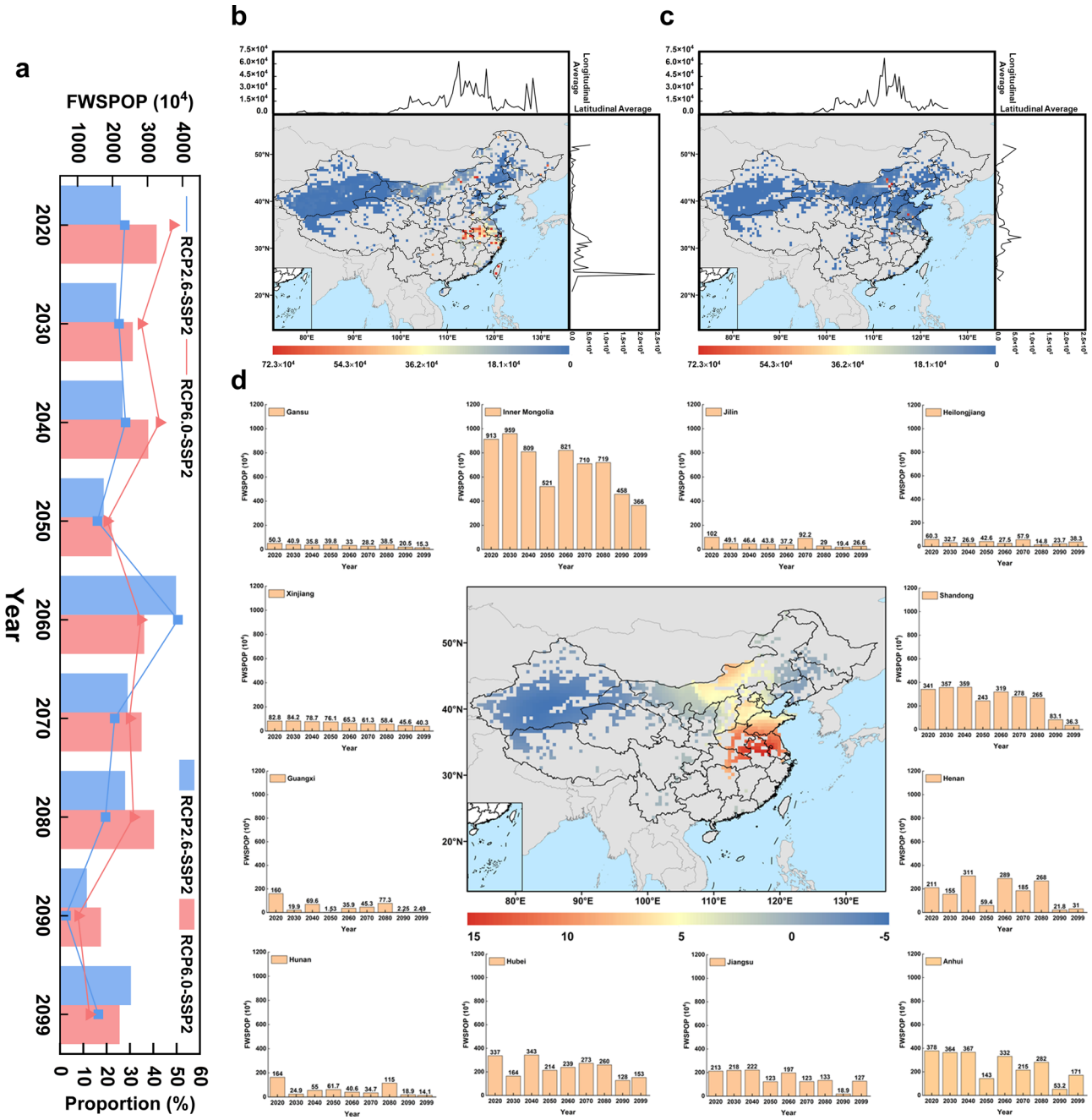

Fig. 5 | Temporal and Spatial variations of water-stressed population. a Temporal variations of FWSPOP. Lines represent the value of FWSPOP. Bars represent FWSPOP as a percentage of the total population. Under both scenarios, on average over 20% of the total population would be water-stressed annually. **b** Spatial distribution of FWSPOP in 2099 under RCP2.6-SSP2 scenario. **c** Spatial distribution of FWSPOP in 2099 under RCP6.0-SSP2 scenario. Under both scenarios, the FWSPOP would mainly be distributed in northern parts of China. **d** Hotspot analysis of FWSPOP under RCP6.0-SSP2 scenario in the late century. FWSPOP hot spots would be mainly located in Beijing, Tianjin, Hebei, Shandong, Henan, Jiangsu and Anhui provinces. The central map represents the spatial distribution of Z-score values from Getis-Ord hotspot analysis. Surrounding bar charts represent the changing trends of FWSPOP in 12 provinces with the highest value of FWSPOP.

Agriculture sector is an essential pillar for China's national economy, with agricultural water consumption accounting for more than 60% of the country's total water usage[43]. Although agricultural production areas have been distributed in all eastern, western, southern and northern parts of China, the most suitable arable land for crop production are mainly located in three alluvial plains: the NCP, the Northeast China Plain (NECP), and the Yangtze Plain (YP)[44], and except for YP, the other two plains are projected to have high water stress, especially the NCP (Fig. 2). As the agricultural base and major producer of crops, NCP provides nearly 50% of China's maize and wheat production[45], but it also consumes more than four times as much water as its total annual renewable water[46]. According to our prediction of future water stress in NCP (Fig. 2), there would be a dilemma for NCP to increase agricultural production while conserving water resources. If irrigation water consumption continues to increase in the NCP, the wet-bulb temperature in the NCP will be greatly increased, which can increase the risks of extreme heatwaves[47]. In turn, the compound dry and hot extremes will further increase the water stress in the NCP, threatening food security[48]. Moreover, it is estimated that under the SSP2 scenario, the value-added of primary industry in the NCP would increase the most[24], which would worsen the water stress of this region. For one thing, addressing water stress

in the NCP could involve enhancing the efficiency of agricultural water use. For instance, under conditions of sufficient soil moisture prior to sowing, implementing two irrigations at the jointing and anthesis stages with an irrigation amount of 150 mm can effectively reduce water usage for irrigation while simultaneously increasing wheat yields in the NCP[49]. Besides, research has demonstrated that a reduced irrigation management practice, which entails no irrigation post-sowing of winter wheat and the sowing of summer maize in June, yields favorable grain output and also enhances water use efficiency in the winter wheat-summer maize rotation system[50]. Additionally, a decade-long field survey has indicated that adopting rotary tillage methods can effectively increase water use efficiency in the NCP area without compromising soil compaction, thereby boosting grain production[51]. For another, China's water resource allocation policies, such as the SNWDP detailed later in the following parts, can effectively alleviate water stress in the northern regions. Furthermore, the geographical distribution of water stress calculated in our study, along with existing research, suggests that a portion of agricultural production could also be feasibly relocated to southern areas where water stress is lower. For example, research indicates that solely improving food production efficiency, optimizing fertilizer utilization, or altering dietary habits cannot reduce the environmental impact of agriculture in the north to within national standards. A feasible supplementary strategy is the reallocation of food production between regions[52,53]. The study by Hu et al. indicates that Henan, Shandong, and Jiangsu provinces in the NCP need to remove more than 20% of their provincial food production to alleviate high water stress and help reduce agricultural environmental impacts within national and provincial boundaries[54]. In turn, the reallocated production amount could be mainly in southern provinces where we estimated to have low water stress (Figs. 2 and 3), namely Fujian, Jiangxi, and Zhejiang, which would increase their production by more than 60%[54]. However, it is worth noting that such a large-scale transfer of agricultural production from north to south would have extensive socio-economic impacts. On one hand, the magnitude of the agricultural transfer merits further exploration in the future to determine how to balance the trade-offs between socioeconomic impacts and water stress alleviation. On the other hand, it is also necessary to gradually promote the shift of agriculture from north to south in a phased manner.

The uneven spatial distribution of water stress in China could also trigger manufacturing industry to migrate from north to south. Manufacturing industry has developed rapidly in China, with most manufacturing firms and labor concentrated in the Beijing-Tianjin-Hebei region (BTH), the Yangtze River Delta (YRD), and Pearl River Delta (PRD), and Shandong Peninsula (SP)[55,56], among which, the BTH and SP were projected to have high water stress in the future (Figs. 2 and 3). Due to the increasing cost of land and labor, and the changes of policy, the labor-intensive manufacturing firms have migrated from these eastern coastal regions to inland China, such as Chengdu and Chongqing[56–59], where water stress were estimated to be comparatively low (Figs. 2 and 3). Meanwhile, many of the labor-intensive industries have also been moved out of China to less-developed Southeast Asian countries, thus giving rooms for the development of high-tech and capital-intensive industries, especially the semiconductor industry[60]. China has initiated the *National Long-term Scientific and Technological Development Plan (2006-2020)* to improve the technology of semiconductor industry[61]. To strengthen this development, the *Fourteenth Five-Year Plan (2021-2025)* further highlighted the necessity of developing the third generation semiconductor materials. These all indicate that semiconductor manufacturing scale will continue to increase in the future, but consequently, the water stress in BTH, SP will also increase. Semiconductor industry is estimated to be a large consumer of fresh water, whose water use approximately accounts for over 27% of the total industry water use in China[62]. In 2021, the mean water use of semiconductor corporations in China was estimated to be 8.22 L/cm^2 [63]. Under the SSP2 scenario, in 2100, the secondary industry is estimated to be concentrated more in the BTH and SP regions compared to 2015[24]. Considering the huge water consumption of semiconductor industry, the BTH and SP regions will suffer from increasingly high water stress, which might in turn impede the development of semiconductor industry. Therefore, to avoid the increasing water stress concerns, manufacturing industries, especially the semiconductor industry, could be partly reallocated from BTH and SP to southern regions with low water stress such as Chengdu, Chongqing and PRD.

Driven by uneven spatial distribution of water stress, it is likely that some Chinese population would migrate from highly water-stressed northern provinces to less water-stressed southern provinces. First, along with the north-to-south migration of agriculture and manufacturing sectors, correspondingly, the labor force of each industry will also migrate among provinces. Second, climate change is also a reason for population migration[64]. Thus, according to our calculations, the increasing water stress due to climate change could also be a driving factor for the migration of some populations from the north to the south. According to our prediction results (Fig. 5), more than 20% of the Chinese population would be under severe water stress every year under both RCP2.6-SSP2 and RCP6.0-SSP2 scenarios, which would be located in the north and northwest of China. As a result, it is quite likely that some risk-averse people will migrate to the south from the north and northwest in the future in the face of high water stress. Specifically, according to our estimation results and discussion above, with the potential migration of agriculture due to the uneven spatial distribution of water stress, agricultural labor might move from Beijing, Tianjin, Hebei, Henan, Shandong and Shanxi to southern provinces such as Zhejiang, Fujian and Jiangxi. And with the potential provincial migration of manufacturing, manufacturing labor will also be likely to move from Beijing, Tianjin, Hebei and Shandong provinces to Chongqing, Sichuan and Guangdong. To sum up, water-stressed population might mainly migrate from Beijing, Tianjin, Hebei, and Shandong to Fujian and Guangdong. It is estimated that the percentage of immigrants migrating to Fujian and Guangdong would exceed 30% of these region's total population[64].

It is worth noting that water stress can be one of the important factors that drive inter-regional population migration, but not the only factor. Other determinants of migration include wages, job opportunities, air pollution, personal preference, agglomeration effect, family factors etc[65–67]. But the most obvious benefit of the north-to-south population migration is that those under severe water stress will have more abundant water resources. Meanwhile, because the destinations to which these populations migrate are not only less water-stressed, but also have smaller environmental health burdens and developed economies[68], the overall social welfare of the migrating population will be increased. In addition, the north-to-south migration can help to alleviate the pressure of the ecosystem and improve the vegetation conditions in the northern provinces[69]. However, population migration is also accompanied by some negative environmental impacts. For example, due to population migration, both provinces with net outward and inward population migration will suffer from increases in carbon emissions and carbon reduction barriers[70,71]. Moreover, studies have shown that every additional 10,000 interprovincial population migrants will result in a 0.2-0.5% increase in COD, a 0.10-0.20% increase in SO_2, and a 3.1-4.2% increase in aggregate waste disposed[72]. Therefore, although population migration could be a means to relieve the high water stress suffered by the northern population, the trade-offs of population migration need to be further controlled.

To alleviate the increasing water stress and address the inequity caused by uneven water stress distribution, the following solutions are available: the further implementation of south-to-north water diversion, and the promotion of industrial migration. The SNWDP is essential in addressing the disparity in water resources distribution between the north and south. This water diversion project has three routes (the eastern, central and western routes)[73,74], and once the three routes are all completed, the SNWDP can transfer up to 44.8×10^9 m^3 freshwater from the south to the north per year, and over 300 million people will benefit from this project. Although the SNWDP has helped to reduce inequities between north and south in terms of water resources, there are still many northern provinces that have not benefited from this project, since it is still under construction. Besides, the large scale of water diversion could generate adverse impacts on water

quality and ecosystem in both the receiving and donating river basins[75–77]. Therefore, to promote the water diversion from south to north, the construction of eastern and western routes needs to be continued and more efforts should be taken to address water pollution issues. SNWDP alone is not enough. According to our discussion of the potential north-to-south migration of agriculture and manufacturing sectors, the key may lie in promoting the production of agriculture and manufacturing sectors in the south, thus helping northern provinces reduce water consumption. An important reason why agriculture in China is currently concentrated in the north for large-scale production is that the terrain in the north is flat, which is suitable for large-scale farming, so even though there is a mismatch between poor water resource and high water consumption, the north is still by far the most suitable region for food production. In contrast, the south, especially the southern hilly areas, is not suitable for large-scale agricultural production. The hilly areas have a lot of sloping land and scattered small plots, so farming machinery operations, and transportation receive considerable restrictions. Therefore, in the future, land consolidation could be further promoted to integrate the scattered small plots of land in the south, and at the same time, make the hilly mountainous areas more suitable for mechanization. Furthermore, considering the climatic characteristics of the south, expanding agricultural production could involve promoting rice cultivation. For example, the development of deep-water rice cultivation techniques could enhance rice's adaptability to floods. Leveraging the south's biodiversity advantage could also reduce the use of chemical pesticides in crop production, thereby fostering the sustainable development of the agricultural ecosystem. In terms of policy, government support for agriculture and poverty alleviation policies should also play an important role in advancing agricultural development in the south. By doing so, the agriculture production could be improved in the south, laying more possibilities for alleviating future water stress in the north. For the manufacturing sector, China is currently undergoing an upgrading transformation of its manufacturing industry, as evidenced by the gradual relocation of labor-intensive industries to Southeast Asia and the booming of capital-intensive industries such as semiconductor manufacturing. To promote these high-tech and high water-consuming manufacturing industries migrate from the north to the south, on the one hand, more stringent industrial environmental regulations should be implemented in the north, and on the other hand, more attractive policies should be enacted in the south, such as Chongqing, Chengdu, and the Pearl River Delta region, all of which require close cooperation and collaboration with local governments.

Methods

Study approach

In this study, we developed the FTOPWSP index to project spatiotemporal water stress variations in China. Firstly, considering the representativeness and accessibility of data, we selected ten indexes from the demand and supply sides as driving factors of water stress changes. Following this, we utilized the principal component analysis (PCA) and entropy weight method (EWM) to estimate the combined weight of each index. Combining the impacts of ten indexes, we developed the FTOPWSP index by using the fuzzy TOPSIS method. This approach has been widely used in recent decades to solve problems related to multi-criteria decision analysis in various fuzzy environments[78–80]. The larger the value of the FTOPWSP index, the greater the level of water stress. Furthermore, we developed the FWSPOP index to measure the social impacts of water stress fluctuations by estimating the population under severe water stress.

The development of WDSIs

Considering the selection of water resources demand and supply indexes (WDSIs) in current studies[13,16,77] and the availability of data, we established a WDSIs system consisting of ten indexes (Table 1 and Supplementary Fig. 7). The water resources demand side contains four indexes representing human consumption and natural evapotranspiration. And the water resources supply side includes six indexes representing natural replenishment. For the properties of these indexes, + represents a positive index, the increase of which will contribute to the decrease in water stress; while - represents a negative index, the increase of which will contribute to the increase in water stress.

Table. 1 | Water resources demand and supply index system

System	Category	Indexes	Symbol	Property
Water demand and supply index system	Demand side	Domestic water withdrawal	X_1	-
		Irrigation water withdrawal	X_2	-
		Manufacturing water withdrawal	X_3	-
		Evapotranspiration	X_4	-
	Supply side	Groundwater runoff	X_5	+
		Groundwater recharge resources	X_6	+
		Surface runoff	X_7	+
		Subsurface runoff	X_8	+
		Total soil moisture content	X_9	+
		Snow water equivalent	X_{10}	+

Principal component analysis (PCA) and entropy weight method (EWM) were utilized to calculate the combination weight ω_j of each index (Supplementary Methods), so as to reduce the interference from subjective judgment factors and avoid the deviation between the weight determined by the simple objective method and the actual importance of indexes.

Development of FTOPWSP and FWSPOP index

The fuzzy TOPSIS method is utilized to develop FTOPWSP index. Explaining the reasons for water stress variations is similar to identifying the influence of different water supply and demand factors, which is logically consistent with the ranking of multiple alternatives in the multi-criteria problem, therefore, the TOPSIS method can be used to reconstruct the water stress index and explain the causes for the variations of water stress. However, the TOPSIS method cannot avoid the bias caused by the uncertainty of data in the calculation process[81]. Therefore, we adopt the fuzzy TOPSIS method to calculate water stress variations[82]. To estimate water stress, the first step is the construction of the fuzzy decision matrix. For a certain period, the value of the j th index in the i th unit grid (0.5° × 0.5°) is set as t_{ij}:

$$t_{ij} = (a_{ij}, b_{ij}, c_{ij}) \tag{1}$$

where a_{ij}, b_{ij}, and c_{ij} represents the different values of the same water supply and demand index calculated by the same WRPMs under the GFDL-ESM2M, HadGEM2-ES, and MIROC5 general circulation models (GCMs), respectively. We applied three WRPMs, namely the H08 model, CWatM, and PCR-GLOBWB model, to obtain the data of the water supply and demand index under the aforementioned three GCMs to enhance the robustness of the calculation results. The fuzzy decision matrix $T = (t_{ij})_{m\times n}$ is then represented as follows:

$$T = \begin{bmatrix} t_{11} & t_{12} & \cdots & t_{1n} \\ t_{21} & t_{22} & \cdots & t_{2n} \\ \vdots & \vdots & \ddots & \vdots \\ t_{m1} & t_{m2} & \cdots & t_{mn} \end{bmatrix} \tag{2}$$

Next step is the normalization of the fuzzy decision matrix. The normalized values are calculated by min-max method:

$$r_{ij} = \left(\frac{a_{ij} - a_{min}}{a_{\max} - a_{min}} \quad \frac{b_{ij} - b_{min}}{b_{\max} - b_{min}} \quad \frac{c_{ij} - c_{min}}{c_{\max} - c_{min}} \right) \tag{3}$$

After the normalization of fuzzy decision matrix, we calculated the weighted normalized fuzzy decision matrix:

$$v_{ij} = r_{ij} \times \omega_j \tag{4}$$

$$V = [v_{ij}]_{m \times n} \tag{5}$$

where ω_j is the weight of the j th water stress index determined by both PCA and EWM (Supplementary Table 1), and V represents the weighted normalized fuzzy decision matrix.

For fuzzy TOPSIS method, the evaluation basis of the optimal solution is that under the benefit standard the geometric distance between the solution and the positive-ideal solution (PIS) is the shortest, and under the cost standard the distance between the solution and the negative-ideal solution (NIS) is the longest. Therefore, we calculated the fuzzy positive-ideal solution (FPIS, A^+) and the fuzzy negative-ideal solution (FNIS, A^-):

$$A^+ = (v_1^+, v_2^+, \cdots, v_n^+) \text{ where } v_j^+ = \max_i \{v_{ij}\} \tag{6}$$

$$A^- = (v_1^-, v_2^-, \cdots, v_n^-) \text{ where } v_j^- = \min_i \{v_{ij}\} \tag{7}$$

where v^+_j and v^-_j are the maximum and minimum values of weighted normalized fuzzy numbers of the j th water stress index in all unit grids from 2020 to 2099.

We then set $d_v(G, H)$ as the distance between two fuzzy number:

$$G = (g_1, g_2, g_3) \tag{8}$$

$$H = (h_1, h_2, h_3) \tag{9}$$

$$d_v(G, H) = \sqrt{1/3[(g_1 - h_1)^2 + (g_2 - h_2)^2 + (g_3 - h_3)^2]} \tag{10}$$

According to the above calculation formula, $d_v(v_{ij}, v_j^+)$ and $d_v(v_{ij}, v_j^-)$ can be obtained, which represent the distance of each water demand and supply index from FPIS and FNIS respectively. The total positive distance d_i^+ and total negative distance d_i^- for each unit grid are obtained by summing the distances of all indexes in each unit grid:

$$d_i^+ = \sum_{j=1}^{n} d_v(v_{ij}, v_j^+) \tag{11}$$

$$d_i^- = \sum_{j=1}^{n} d_v(v_{ij}, v_j^-) \tag{12}$$

According to the positive and negative distances, the FTOPWSP index can be constructed as follows:

$$FTOPWSP_i = \frac{d_i^+}{d_i^+ + d_i^-} \tag{13}$$

For a certain period, the larger the FTOPWSP index of a region is, the farther the water stress of the region is to the optimal status, namely, the larger the water stress of the region is. For a certain region, the temporal changing trend of water stress can be identified by calculating the variations of water stress in each time step in the future. Combining the predictions of temporal and spatial variation trends, we analyzed the overall changing characteristics of water stress in China in the future 80 years. In the calculation of the FTOPWSP, we use a monthly time step and a spatial resolution of 0.5° × 0.5° grid cells.

According to the FTOPWSP index prediction results, the social impact of water stress variations in China is quantified by calculating the number of people under severe water stress. In this study, we utilized the 60th percentile as the threshold to calculate the water-stressed population (FWSPOP). That is, the population within unit grids where the FTOPWSP value is at the 60th percentile or above is considered FWSPOP. In the Supplementary Fig. 4, we provided calculation results for different thresholds, namely the 50th, 60th, 70th, 80th, and 90th percentiles. By comparing the FWSPOP population distribution across different thresholds, we found that the 60th percentile serves as the most rational and moderate threshold for the calculation results.

Data availability

The data involved in this study include historical data and future prediction data. For historical data, China's administrative boundary vector data is obtained from the National Earth System Science Data Center (http://www.geodata.cn). For future projections, the population data is selected from the Global One-Eighth Degree Population Base Year and Projection Grids Based on the SSPs, v1.01 (2000-2100) dataset in the Socioeconomic Data and Application Center (SEDAC) (https://sedac.ciesin.columbia.edu/data/set/popdynamics-1-8th-pop-base-year-projection-ssp-2000-2100-rev01). Given data availability, we adopted the SSP2 population data. Monthly data of water demand and supply from 2020 to 2099 is provided by the Inter-Sectoral Impact Model Intercomparison Project phase 2b (ISIMIP 2b) (https://data.isimip.org/search/tree/ISIMIP2b/). These simulations were performed by H08, CwatM, and PCR-GLOBWB models driven by three GCMs, namely, GFDL-ESM2M, HadGEM2-ES and MIROC5 with a spatial resolution of 0.5°×0.5°. To leverage more data, we utilized projection data from the aforementioned models under scenarios with fixed year-2005 land use, nitrogen deposition, and fertilizer input. The IPSL-CM5A-LR GCM model is not incorporated in our calculation because it has a persistent cold bias in its temperature simulations, which affects its overall climate projections[83]. Data created in this study are openly available which can be found in Figshare repository with the https://doi.org/10.6084/m9.figshare.26054476.v1[84].

Code availability

Code to calculate the FTOPWSP index can be found in Github repository with the identifier https://github.com/Mengyu-Liu/FTOPWSP_index_calculation.

Received: 9 November 2023; Accepted: 9 July 2024;
Published online: 23 July 2024

References

1. Vörösmarty, C. J. et al. Global threats to human water security and river biodiversity. *nature* **467**, 555–561 (2010).
2. Wada, Y., Van Beek, L. & Bierkens, M. F. Modelling global water stress of the recent past: on the relative importance of trends in water demand and climate variability. *Hydrology and Earth System Sciences* **15**, 3785–3808 (2011).
3. Schewe, J. et al. Multimodel assessment of water scarcity under climate change. *Proceedings of the National Academy of Sciences* **111**, 3245–3250 (2014).
4. Greve, P. et al. Global assessment of water challenges under uncertainty in water scarcity projections. *Nature Sustainability* **1**, 486–494 (2018).
5. Huang, J., Yu, H., Dai, A., Wei, Y. & Kang, L. Drylands face potential threat under 2 C global warming target. *Nature Climate Change* **7**, 417–422 (2017).

6. Gudmundsson, L., Seneviratne, S. I. & Zhang, X. Anthropogenic climate change detected in European renewable freshwater resources. *Nature Climate Change* **7**, 813–816 (2017).
7. Flörke, M., Schneider, C. & McDonald, R. I. Water competition between cities and agriculture driven by climate change and urban growth. *Nature Sustainability* **1**, 51–58 (2018).
8. Yin, Y., Tang, Q., Liu, X. & Zhang, X. Water scarcity under various socio-economic pathways and its potential effects on food production in the Yellow River basin. *Hydrology and Earth System Sciences* **21**, 791–804 (2017).
9. Xu, M., Li, C., Wang, X., Cai, Y. & Yue, W. Optimal water utilization and allocation in industrial sectors based on water footprint accounting in Dalian City, China. *Journal of cleaner production* **176**, 1283–1291 (2018).
10. Vörösmarty, C. J., Douglas, E. M., Green, P. A. & Revenga, C. Geospatial indicators of emerging water stress: an application to Africa. *AMBIO: A journal of the Human Environment* **34**, 230–236 (2005).
11. Hanasaki, N. et al. A global water scarcity assessment under Shared Socio-economic Pathways–Part 2: Water availability and scarcity. *Hydrology and Earth System Sciences* **17**, 2393–2413 (2013).
12. Mekonnen, M. M. & Hoekstra, A. Y. Four billion people facing severe water scarcity. *Science advances* **2**, e1500323 (2016).
13. Liu, X. et al. A spatially explicit assessment of growing water stress in China from the past to the future. *Earth's Future* **7**, 1027–1043 (2019).
14. Munia, H. A. et al. Future transboundary water stress and its drivers under climate change: a global study. *Earth's future* **8**, e2019EF001321 (2020).
15. He, C. et al. Future global urban water scarcity and potential solutions. *Nature Communications* **12**, 4667 (2021).
16. Liu, X. et al. Global agricultural water scarcity assessment incorporating blue and green water availability under future climate change. *Earth's Future* **10**, e2021EF002567 (2022).
17. Ge, L. et al. An evaluation of China's water footprint. *Water Resources Management* **25**, 2633–2647 (2011).
18. Sun, S., Fang, C. & Lv, J. Spatial inequality of water footprint in China: A detailed decomposition of inequality from water use types and drivers. *Journal of Hydrology* **553**, 398–407 (2017).
19. Cheng, H., Hu, Y. & Zhao, J. Meeting China's water shortage crisis: current practices and challenges. *Environmental science & technology* **43**, 240–244 (2009).
20. Jiang, Y. China's water security: current status, emerging challenges and future prospects. *Environmental Science & Policy* **54**, 106–125 (2015).
21. Liu, Y. et al. Agriculture intensifies soil moisture decline in Northern China. *Scientific reports* **5**, 11261 (2015).
22. Wang, X. et al. Impact of the changing area sown to winter wheat on crop water footprint in the North China Plain. *Ecological Indicators* **57**, 100–109 (2015).
23. Wang, E., Yu, Q., Wu, D. & Xia, J. Climate, agricultural production and hydrological balance in the North China Plain. *International Journal of Climatology: A Journal of the Royal Meteorological Society* **28**, 1959–1970 (2008).
24. Jing, C. et al. Gridded value-added of primary, secondary and tertiary industries in China under Shard Socioeconomic Pathways. *Scientific Data* **9**, 309 (2022).
25. Jin, L. & Young, W. Water use in agriculture in China: importance, challenges, and implications for policy. *Water policy* **3**, 215–228 (2001).
26. Man, Y. et al. Woods to goods: Water consumption analysis for papermaking industry in China. *Journal of Cleaner Production* **195**, 1377–1388 (2018).
27. Kang, S. et al. Improving agricultural water productivity to ensure food security in China under changing environment: From research to practice. *Agricultural Water Management* **179**, 5–17 (2017).
28. Liu, Y. & Zhang, X. Does labor mobility follow the inter-regional transfer of labor-intensive manufacturing? The spatial choices of China's migrant workers. *Habitat International* **124**, 102559 (2022).
29. Han, J., Li, G., Shen, Z., Song, M. & Zhao, X. Manufacturing transfer and environmental efficiency: Evidence from the spatial agglomeration of manufacturing in China. *Journal of Environmental Management* **314**, 115039 (2022).
30. Kuzma, S. et al. *Aqueduct 4.0: Updated decision-relevant global water risk indicators*. World Resources Institute Washington, DC, USA (2023).
31. Pritchard, H. D. Asia's shrinking glaciers protect large populations from drought stress. *Nature* **569**, 649–654 (2019).
32. Immerzeel, W. W. et al. Importance and vulnerability of the world's water towers. *Nature* **577**, 364–369 (2020).
33. Yao, T. et al. The imbalance of the Asian water tower. *Nature Reviews Earth & Environment* **3**, 618–632 (2022).
34. Zhang, Q. et al. Oceanic climate changes threaten the sustainability of Asia's water tower. *Nature* **615**, 87–93 (2023).
35. Piao, S. et al. The impacts of climate change on water resources and agriculture in China. *Nature* **467**, 43–51 (2010).
36. Yin, Y. et al. Quantifying Water Scarcity in Northern China Within the Context of Climatic and Societal Changes and South-to-North Water Diversion. *Earth's Future* **8**, e2020EF001492 (2020).
37. Ma, T. et al. Pollution exacerbates China's water scarcity and its regional inequality. *Nature communications* **11**, 650 (2020).
38. Chen, C.-T. Extensions of the TOPSIS for group decision-making under fuzzy environment. *Fuzzy sets and systems* **114**, 1–9 (2000).
39. Hanasaki, N., Yoshikawa, S., Pokhrel, Y. & Kanae, S. A global hydrological simulation to specify the sources of water used by humans. *Hydrology and Earth System Sciences* **22**, 789–817 (2018).
40. Boulange, J., Yoshida, T., Nishina, K., Okada, M. & Hanasaki, N. Delivering the latest global water resource simulation results to the public. *Climate Services* **30**, 100386 (2023).
41. Burek, P. et al. Development of the Community Water Model (CWatM v1. 04)–a high-resolution hydrological model for global and regional assessment of integrated water resources management. *Geoscientific Model Development* **13**, 3267–3298 (2020).
42. Sutanudjaja, E. H. et al. PCR-GLOBWB 2: a 5 arcmin global hydrological and water resources model. *Geoscientific Model Development* **11**, 2429–2453 (2018).
43. An, Y., Li, Q. & Zhang, L. Managing Agricultural Water Use in a Changing Climate in China. *Sustainable Production and Consumption* **33**, 978–990 (2022).
44. Shi, YL Y. Y. & Shi, Z. J., eds. *Land resources map of China (in Chinese)*. China Land Press (2006).
45. Qin, W., Wang, D., Guo, X., Yang, T. & Oenema, O. Productivity and sustainability of rainfed wheat-soybean system in the North China Plain: results from a long-term experiment and crop modelling. *Scientific reports* **5**, 1–16 (2015).
46. Xu, Z. et al. Impacts of irrigated agriculture on food–energy–water–CO2 nexus across metacoupled systems. *Nature communications* **11**, 5837 (2020).
47. Kang, S. & Eltahir, E. A. North China Plain threatened by deadly heatwaves due to climate change and irrigation. *Nature communications* **9**, 2894 (2018).
48. Zhang, Y., Hao, Z. & Zhang, Y. Agricultural risk assessment of compound dry and hot events in China. *Agricultural Water Management* **277**, 108128 (2023).
49. Xu, X. et al. Improving water use efficiency and grain yield of winter wheat by optimizing irrigations in the North China Plain. *Field Crops Research* **221**, 219–227 (2018).
50. Wang, Y. et al. Reduced irrigation increases the water use efficiency and productivity of winter wheat-summer maize rotation on the North China Plain. *Science of the Total Environment* **618**, 112–120 (2018).

51. Kan, Z.-R. et al. Responses of grain yield and water use efficiency of winter wheat to tillage in the North China Plain. *Field Crops Research* **249**, 107760 (2020).
52. Zou, J., Fu, S.-T., Yang, Y.-R. & Mao, D.-H. Spatial optimization of agricultural regions under the background of virtual water strategy. *Resources and Environment in the Yangtze Basin* **19**, 1427–1432 (2010).
53. Davis, K. F., Rulli, M. C., Seveso, A. & D'Odorico, P. Increased food production and reduced water use through optimized crop distribution. *Nature Geoscience* **10**, 919–924 (2017).
54. Hu, Y. et al. Food production in China requires intensified measures to be consistent with national and provincial environmental boundaries. *Nature Food* **1**, 572–582 (2020).
55. He, C., Wei, Y. D. & Pan, F. Geographical concentration of manufacturing industries in China: The importance of spatial and industrial scales. *Eurasian Geography and Economics* **48**, 603–625 (2007).
56. Fan, C. et al. China's Gridded Manufacturing Dataset. *Scientific Data* **9**, 742 (2022).
57. Wu J., Cui C., Mei X., Xu Q., Zhang P. Migration of manufacturing industries and transfer of carbon emissions embodied in trade: empirical evidence from China and Thailand. *Environmental Science and Pollution Research*, 1-13 (2021).
58. Yang, C. Relocating labour-intensive manufacturing firms from China to Southeast Asia: A preliminary investigation. *Bandung* **3**, 1–13 (2016).
59. He, C. & Wang, J. Regional and sectoral differences in the spatial restructuring of Chinese manufacturing industries during the post-WTO period. *GeoJournal* **77**, 361–381 (2012).
60. Kong, X. X., Zhang, M. & Ramu, S. C. China's semiconductor industry in global value chains. *Asia Pacific Business Review* **22**, 150–164 (2016).
61. Li, H., He, H., Shan, J. & Cai, J. Innovation efficiency of semiconductor industry in China: A new framework based on generalized three-stage DEA analysis. *Socio-Economic Planning Sciences* **66**, 136–148 (2019).
62. Frost K., Hua I. A spatially explicit assessment of water use by the global semiconductor industry. In: *2017 IEEE Conference on Technologies for Sustainability (SusTech)*). IEEE (2017).
63. Wang, Q. et al. Environmental data and facts in the semiconductor manufacturing industry: An unexpected high water and energy consumption situation. *Water Cycle* **4**, 47–54 (2023).
64. Sun Y., Xu C., Zhang H., Wang Z. Migration in response to climate change and its impact in China. *International Journal of Climate Change Strategies and Management*, (2017).
65. Chan, S. Spatial lock-in: do falling house prices constrain residential mobility? *Journal of urban Economics* **49**, 567–586 (2001).
66. Chen, S., Oliva, P. & Zhang, P. The effect of air pollution on migration: evidence from China. *Journal of Development Economics* **156**, 102833 (2022).
67. Crozet, M. Do migrants follow market potentials? An estimation of a new economic geography model. *Journal of Economic geography* **4**, 439–458 (2004).
68. Lin, A. et al. Changes in the PM2. 5-related environmental health burden caused by population migration and policy implications. *Journal of Cleaner Production* **287**, 125051 (2021).
69. Qu, S., Wang, L., Lin, A., Zhu, H. & Yuan, M. What drives the vegetation restoration in Yangtze River basin, China: climate change or anthropogenic factors? *Ecological Indicators* **90**, 438–450 (2018).
70. Bu, Y., Wang, E., Qiu, Y. & Möst, D. Impact assessment of population migration on energy consumption and carbon emissions in China: A spatial econometric investigation. *Environmental Impact Assessment Review* **93**, 106744 (2022).
71. Qi, W. & Li, G. Residential carbon emission embedded in China's inter-provincial population migration. *Energy Policy* **136**, 111065 (2020).
72. Rafiq, S., Nielsen, I. & Smyth, R. Effect of internal migration on the environment in China. *Energy Economics* **64**, 31–44 (2017).
73. Liu, C. & Zheng, H. South-to-north water transfer schemes for China. *International Journal of Water Resources Development* **18**, 453–471 (2002).
74. Zhang, Q. The South-to-North Water Transfer Project of China: Environmental Implications and Monitoring Strategy 1. *JAWRA Journal of the American Water Resources Association* **45**, 1238–1247 (2009).
75. Gohari, A. et al. Water transfer as a solution to water shortage: a fix that can backfire. *Journal of Hydrology* **491**, 23–39 (2013).
76. Guo, C. et al. Eutrophication and heavy metal pollution patterns in the water suppling lakes of China's south-to-north water diversion project. *Science of The Total Environment* **711**, 134543 (2020).
77. Qu, X. et al. A holistic assessment of water quality condition and spatiotemporal patterns in impounded lakes along the eastern route of China's South-to-North water diversion project. *Water Research* **185**, 116275 (2020).
78. Gündoğdu, F. K. & Kahraman, C. A novel fuzzy TOPSIS method using emerging interval-valued spherical fuzzy sets. *Engineering Applications of Artificial Intelligence* **85**, 307–323 (2019).
79. Lee, G., Jun, K. S. & Chung, E.-S. Robust spatial flood vulnerability assessment for Han River using fuzzy TOPSIS with α-cut level set. *Expert Systems with Applications* **41**, 644–654 (2014).
80. Zyoud, S. H., Kaufmann, L. G., Shaheen, H., Samhan, S. & Fuchs-Hanusch, D. A framework for water loss management in developing countries under fuzzy environment: Integration of Fuzzy AHP with Fuzzy TOPSIS. *Expert Systems with Applications* **61**, 86–105 (2016).
81. Zadeh, L. A. Fuzzy logic, neural networks, and soft computing. In: *Fuzzy sets, fuzzy logic, and fuzzy systems: selected papers by Lotfi A Zadeh*). World Scientific (1996).
82. Kutlu Gündoğdu, F. & Kahraman, C. Spherical fuzzy sets and spherical fuzzy TOPSIS method. *Journal of intelligent & fuzzy systems* **36**, 337–352 (2019).
83. Dufresne, J.-L. et al. Climate change projections using the IPSL-CM5 Earth System Model: from CMIP3 to CMIP5. *Climate dynamics* **40**, 2123–2165 (2013).
84. Liu, M. Processes data for graphs and charts_the increasing water stress projected for China could shift the agriculture and manufacturing industry geographically.xlsx.). figshare (2024).

Acknowledgements

This research is supported by the by the Natural Science Foundation of China (NSFC) Project (U2243236, 51779008, U2040212), the special fund of State Key Joint Laboratory of Environment Simulation and Pollution Control, the Fundamental Research Funds for the Central Universities, and the Qinghai Haidong Urban-Rural Eco Development (L3443-PRC-HD-CB-CS4) Project.

Author contributions

M.L. and X.Z. designed the research and wrote the manuscript. M.L. performed the analysis. G.H., Y.L., and X.Z. discussed and revised the manuscript. All authors contributed to the interpretation of results.

Competing interests

The authors declare no competing interests.

Additional information

Supplementary information The online version contains supplementary material available at https://doi.org/10.1038/s43247-024-01560-y.

Correspondence and requests for materials should be addressed to Xiong Zhou.

Peer review information *Communications Earth & Environment* thanks the anonymous reviewers for their contribution to the peer review of this work. Primary Handling Editors: Rahim Barzegar and Martina Grecequet. A peer review file is available.

Reprints and permissions information is available at http://www.nature.com/reprints

Publisher's note Springer Nature remains neutral with regard to jurisdictional claims in published maps and institutional affiliations.

Open Access This article is licensed under a Creative Commons Attribution 4.0 International License, which permits use, sharing, adaptation, distribution and reproduction in any medium or format, as long as you give appropriate credit to the original author(s) and the source, provide a link to the Creative Commons licence, and indicate if changes were made. The images or other third party material in this article are included in the article's Creative Commons licence, unless indicated otherwise in a credit line to the material. If material is not included in the article's Creative Commons licence and your intended use is not permitted by statutory regulation or exceeds the permitted use, you will need to obtain permission directly from the copyright holder. To view a copy of this licence, visit http://creativecommons.org/licenses/by/4.0/.

© The Author(s) 2024